



Smart Small Cell with Hybrid Beam forming for 5G: Theoretical Feasibility and Prototype Results

Mr. Chavan Rahul Raghunath¹, Mr. Chavan Rahul Barama²

HOD, Electronics and Telecommunication Department, AITP, Vita, India¹

Lecturer, Electronics and Telecommunication Department, AITP, Vita, India²

Abstract: In this article, we present a real-time three-dimensional (3D) hybrid beam forming for fifth generation (5G) wireless networks. One of the key concepts in 5G cellular systems is the small cell network, which settles the high mobile traffic demand and provides uniform user-experienced data rates. The overall capacity of the small cell network can be enhanced with the enabling technology of 3D hybrid beam forming. This study validates the feasibility of the 3D hybrid beam forming, mostly for link-level performances, through the implementation of a real-time tested using a software-defined radio (SDR) platform and fabricated antenna array. Based on the measured data, we also investigate system-level performances to verify the gain of the proposed smart small cell system over long term evolution (LTE) systems by performing system-level simulations based on a 3D ray-tracing tool.

Keywords: Small cell, three-dimensional (3D) hybrid beam forming, fifth generation (5G) communications.

I. INTRODUCTION

For the past several years, fifth generation (5G) wireless communication has been actively discussed both in academia and the industry as a means of providing various mobile convergence services. Many 5G project groups have been established to propose service scenarios and target performance metrics. In the coming years, the amount of mobile data traffic is expected to increase tremendously. Given this fact, one important application that most 5G project groups are likely to support is high data rate communications.

A key enabling technology to support a high data rate service scenario appears to be a small cell network. When a network is in the interference-limited regime, it is known theoretically that spectral efficiency per area increases linearly with the number of small cells. From a spatial domain viewpoint, however, there are huge differences can be found in the wireless channel characteristics of small cell networks (e.g., outdoor-to-indoor or indoor-to-indoor) and those of conventional macro cell networks. Various channel environments may occur in a small cell network, since the space constraint for cell deployment can be greatly mitigated, thanks to the reduced deployment time and cost. The channel conditions are affected dynamically by the relative locations among base stations (BSs) and users. Furthermore, non-uniform cell deployment may cause crucial intercell interference (ICI). What is needed then is not only the densification of the network but also the small cell technologies that reflect the above issue so as to enhance the network performance and to full fill 5G target requirements. In 5G cellular networks, a promising technology is one that exploits three-dimensional (3D) beam control. In practical situations, BSs and users are distributed in 3D space, such as in the urban cell scenarios. As the elevation angle of the ray

propagation becomes influential, the 3D beam forming can increase both the cell average throughput and the 5%tile user throughput. A critical issue in addition to the 3D beam forming design is the performance evaluation method that reflects the 3D space accordingly. When it comes to 3D beam forming gain, more elaborate simulation results may be produced by generating BSs and users in both horizontal and vertical domains rather than considering only a two-dimensional (2D) distribution. As a candidate for the small cell architecture of a 5G small cell network, we propose a smart small cell concept. In Fig. 1(a), the smart small cell system applies a mixture of 3D radio frequency (RF) analog beam forming and baseband digital beam forming—referred to as in this article as 3D hybrid beam forming. It provides user-perspective 3D beam directivity that is appropriate to the channel condition of each user. In order to exploit distinguishable beams at an elevation angle, the smart small cell system uses a 2D antenna array instead of a linear antenna array with a fixed radiation pattern in the vertical domain. When 3D beams among cells conflict, users can still experience a uniform data rate if additional baseband ICI management is applied. Focusing on a hybrid beam forming system, this smart small cell concept is proposed particularly for millimeter wave communications. In the mm-wave communications, a beam forming with a number of antennas is used to overcome the path loss of high frequency and to obtain a practical link budget. We further consider the hybrid analog/digital processing strategy to reduce RF hardware costs and a computational complexity over the full digital beam forming that antenna elements are equipped with separate RF chains. The feasibility of the hybrid beam forming for mm-wave communications has been



extensively evaluated by simulations and prototypes. In most cases, the beam weights are designed with the knowledge of instantaneous or statistical channel state information (CSI) at all antenna elements. This requires sufficient training before data transmission. In this article, we discuss a novel 3D hybrid beam forming scheme designed without the advance knowledge of the CSI of all the antenna elements. We examine the link- and system level performances, through a real-time software-defined radio (SDR) test bed and 3D ray-tracing-based simulations, respectively, of the proposed smart small cell system and the conventional multiple input multiple output (MIMO) system. The results show that the proposed 3D hybrid beam forming system can enhance the area spectral efficiency of the 5G small cell network tremendously, even in the currently used frequency band of cellular systems (under 5 GHz).

the data are transmitted simultaneously over disjoint orthogonal frequency division multiplexing (OFDM) symbols. In the proposed hybrid beam forming, the analog beam forming maximizes the average signal-to-noise-ratio (SNR) of each sub array and the digital beam forming performs Mdimensional MIM Oprocessing with instantaneous CSI (comprising of analog beam weights and wireless channels). It is no trivial task to carry out the joint design of the analog beam forming and the digital beam forming with the absence of the CSI of all antenna elements. Hence we adopt a decoupled design of the analogbeam forming and the digital beam forming. The proposed design for the analog beam weight targets the maximization of the average SNR of each sub array without the CSI of all antenna elements. An iterative algorithm tracking the corresponding beam weight is applied. The proposed scheme only requires the information of the previously used beam weights and the corresponding M-dimensional beam formed base band CSI. For more details, see Section IV-B. After the analog beam weight is computed, the M-dimensional digital beam forming, such as spatial multiplexing and diversity schemes, is applied based on the analogbeam formed baseband CSI, which can be estimated with M RF chains. In this way, the proposed hybrid beam forming requires none of the CSI from the actual MN antennas. Also note that the physical layer of the LTE system can be directly applied without any modification into the proposed hybrid beam forming. The number of antenna elements (MN) is largertanthat ofRF chains(M) inthehybridbeam forming system; nonetheless for the data modulation and demodulation in the baseband the proposed system does not require the information of the analog domain, such as the CSI of MN antenna elements or the beam forming weight. In other words, the MN-dimensional analog processing is transparent to the M-dimensional baseband and the increase of antenna elements does not vary any operation of the baseband processing in the physical layer. In the LTE downlink, several types of RS are providedand each RS pattern is transmitted from an antenna port at the BS. Generally, each antenna port in the conventional LTE system consists of a single directive antenna element or multiple antenna elements using fixed beam forming. According to the antenna port concept of the LTE, each antenna port in the proposed hybrid beam forming system may consist of a subset of sub arrays using user-specific analogbeam forming. In either system, users can only estimate the composite channel of the antenna port regardless of the number of antenna elements making up the antenna port.

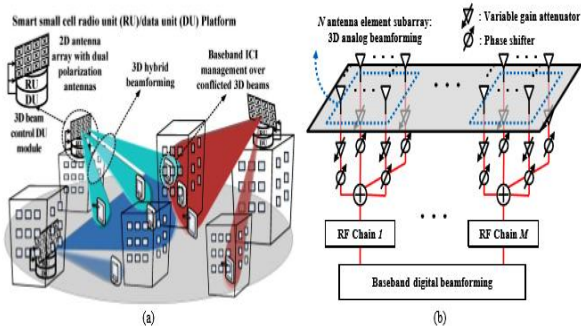


Fig. 1. (a) Smart small cell concept, (b) 3D hybrid beamforming structure.

II. 3D HYBRID BEAMFORMING DESIGN

We consider a 3D hybrid beam forming system, shown in Fig. 1(b), that consists of M RF chains and M sub arrays; a sub array is defined as a subset of antenna elements. The total number of antenna elements is MN, such that each subarray has N antenna elements and is connected to each RF chain (or baseband channel). Note that the number of RF chains and that of antenna elements are the same in the conventional MIMO system whose antenna elements are connected to separate RF chains. A 2D sub array is considered for both vertical and horizontal analogbeam forming, i.e., directive 3D beam forming. In the digital domain, multiple baseband channels can support multiple users, or spatial multiplexing. This can be done through highly directive beam forming by grouping several sub arrays into a virtually large sub array. A conventional hybrid beam forming design assumes perfect knowledge of the instantaneous CSI of all MN antenna elements. Such a design, however, is difficult to implement, as the training duration for sending pilot signals of such a hybrid beam forming system is at least N times longer than that of the conventional MIMO system due to the lack of RF chains. Furthermore, the system is incompatible with currently operating long term evolution (LTE), where it is difficult to estimate the CSI of all antenna elements before data transmission because the reference signal (RS) and

III. TESTBED SETTINGS: SYSTEM SPECIFICATIONS & HARDWARE ARCHITECTURE

The designed real-time hybrid beam forming test bed is based on the LTE standard with the following system specifications: a transmission bandwidth of 20 MHz, 30.72



MHz sampling rate, 15 kHz subcarrier spacing, 2048 fast Fourier transform (FFT) size, and variable 4/16/64 quadrature amplitude modulation (QAM). For this reason, we refer to the test bed as the hybrid beam forming-aided LTE system. Figure 2(a) depicts the implemented prototype; a detailed explanation of the hardware components is given below.

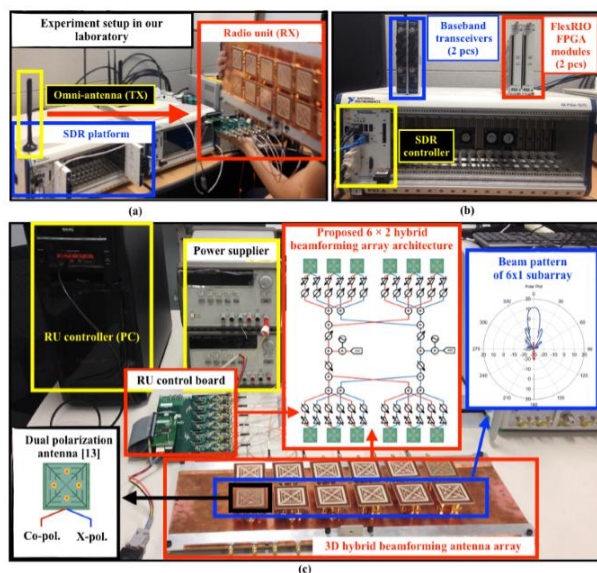


Fig. 2. (a) Real-time hybrid beamforming testbed setup, (b) SDR platform, and (c) RU and supplementary hardware components.

A. Software Defined Radio Platform the SDR platform consists of the following hardware components, shown in Fig. 2(b). • PXIe-8133: Real-time controller equipped with a 1.73 GHz quad-core Intel Core i7-820 processor and 8 GB of dual-channel 1333 MHz DDR3 random access memory (RAM) [10]. • NI 5791R: 100 MHz bandwidth baseband transceiver module equipped with dual 130 MSamples/s analog-to-digital converter (ADC) with 14-bit accuracy, and dual 130 MSamples/s digital-to-analog converter (DAC) with 16-bit accuracy. • PXIe-7965R: Field-programmable gate array (FPGA) module equipped with a Virtex-5 SX95T FPGA optimized for digital signal processing, 512 MB of onboard RAM, and 16 direct memory access (DMA) channels for high-speed data streaming at more than 800 MB/s. In addition, NI modules sit in the NI PXIe-1075 chassis. The chassis is for data aggregation with both FPGA processors and a real-time controller for real-time signal processing.

B. Radio Unit The radio unit (RU) is composed of a 6×2 hybrid beamforming antenna array and an RU control board. Figure 2(c) shows the RU and the supplementary components for measurement, such as the power suppliers and an RU controller (a PC) with a self-designed control program to run the processor embedded in the RU control board. The proposed 3D hybrid beamforming antenna array consists of two 6×2 subarrays based on the dual polarization antenna shown in. The distance between neighbour dual polarization antennas is 0.6λ where λ is the

wavelength. The proposed design groups together 6×2 antenna elements with the same polarization on the RF control board as the sub array and connect them to a single baseband channel. This design reduces the size of the antenna array to half that based on antennas with a single polarization. Since, the 3D radiation patterns of Polarizations 1 and 2 of the dual polarization antenna in are very similar, the beamforming patterns of the subarrays with different polarizations are nearly the same. Most importantly, this antenna gives high cross-polarization discrimination (XPD) in all directions, where XPD is defined as the ratio of the co-polarized average received power to the cross-polarized average received power; it represents the separation of the radiation between Polarization 1 and Polarization 2. High XPD is also shown in Fig. 2(c). The large difference between the main polarization (blue) and sub polarization (red) is seen in all directions implying that in the proposed design sufficiently suppresses the inter-subarray beam interference. The RU control board is designed to control the phase and amplitude of signal input, for upto six antenna elements simultaneously. The following hardware components are included: • ATMEGA2560: 8-bit processor for a 2 MHz channel • MAPS-010144: Phase shifter (PS) of 4-bit quantization (quantization error: 11.25 degree) [6 pcs] • HMC742LP5E: Variable gain attenuator (VGA) of 6-bit quantization (quantization error: 0.25 dB) [6 pcs] • HMC715LP3 (RX RU): Low noise amplifier of 0.9 dB noise figure [6 pcs] • MGA-22003 (TXRU): Power amplifier of 25dB moutput power [6 pcs]. In the RU, it takes approximately tens of μ s time delay at the processor to process the input beam weight and additional hundreds of μ s time delay at the six PSs and VGAs to update the beam weight (tens of μ s time delay per PS and VGA). As a result, 1ms time delay, at most, is required to update the incoming beam weight into the hybrid beamforming antenna array. Such a delay is acceptable in the LTE since the uplink user scheduling is already determined at least 1ms earlier than the actual receiving time.

Note that the system control delay is limited by the Transmission Control Protocol/Internet Protocol (TCP/IP), which is addressed in Section IV and serial-link interface between the SDR receiver and the RU control board. This can be further optimized by implementing all the procedures in the FPGA chip.

IV. REAL-TIME HYBRID BEAMFORMING TESTBED

We now elaborate our design blocks for a real-time 3D hybrid beamforming testbed in a processing order. We assume that there is one transmitter with an omni-antenna and one receiver with a hybrid beam forming antenna array. The number of transmit and receive RF chains is one and the size of the subarray at the receiver is 6×1 . Figure 3 illustrates the block diagram of the implemented test bed. We first briefly introduce main procedure of the



experiment and explain the detailed process of the main blocks in the following subsections:

- 1) The SDR receiver randomly generates an initial beam weight and sends it to the RU controller through TCP/IP.
- 2) The RU controller informs the RU control board of the beam weight, and the RU control board sets the beam weight.
- 3) Transmission and Reception The transmission and the reception are based on the LTE Release 8. An LTE frame has duration of 10 ms and consists of 20 slots.

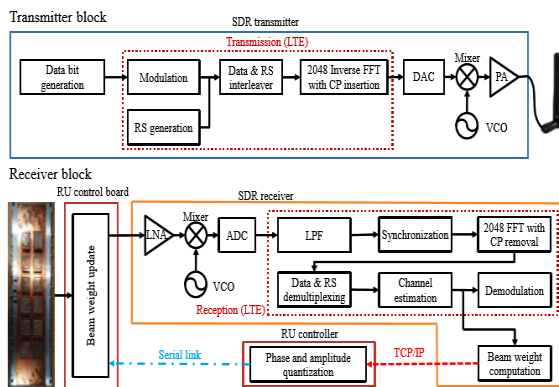


Fig. 3. Block diagram of our real-time hybrid beamforming testbed.

4) Each slot has 0.5 ms of duration and 6 OFDM symbols with an extended cyclic prefix (CP). Although the test link in the SDR testbed is for the uplink, the LTE downlink frame structure is instead used for the simplicity of the testbed, where the RSs and the modulated data symbols are orthogonally mapped to the different subcarriers. The cell-specific RS of Antenna Port 0 in LTE is used. The sixth OFDM symbol of every first and eleventh slot of the frame includes a primary synchronization signal (PSS). Carriers as well as the RS subcarriers. The estimated channel coefficients are passed to the beam weight calculation block (described in the next subsection) and to the demodulation block for the data symbols to be decoded. For data decoding, a single-tap zero-forcing channel equalizer operates in each data subcarrier.

5) Beam Weight Update Procedure in Radio Unit After the beam weight computation is done, the following steps are carried out to update the beam weight in the RU. The real-time controller sends the beam weight to the RU controller through TCP/IP. The RU controller runs the RU control program that has the pre-measured array calibration table, and sends the bit sequences of the quantized phase and amplitude information to the processor of the RU control board. The processor of the RU control board commands PSs and VGAs to update the beam weights. Based on the overall time delay in processing these steps, we define the time period of the beam weight as follows. In Step 1, the measured time delay of TCP/IP per link is 1 ms, then the total time delay of TCP/IP links from the real-time controller to the RU

controller via server becomes $\tau_1 = 2$ ms. In Steps 2 and 3, the measured processing time of the RU control program is, on average, $\tau_2 = 4$ ms. In Step 4, the time delay is $\tau_3 = 1$ ms as mentioned in Section III-B. Overall, the total time delay is $\tau_1 + \tau_2 + \tau_3 = 7$ ms. In a worstcase scenario, the beam-steering operation in RU might take place during an entire half frame since the duration of the half frame in LTE is 5 ms. Hence, we set up the beam update in RU in such a way as to operate every 3 half frames (15 ms), abandoning the two half frames prior to data decoding so as to avoid the error in the beam transition time of the RU. Although the proposed algorithm is designed to update the beam weight at every subframe (i.e., 1 subframe per iteration), a longer period is used in the SDR testbed to avoid errors caused.

6) Average received SNR [dB] Testbed measurement / WiSE Conventional LTE with directional antennas Hybrid beamforming-aided LTE Spot A 16.06 / 18.53 20.06 / 23.11 Spot B 19.13 / 22.04 23.84 / 26.61 enough to meet the 5G requirements; the purpose of this SDR testbed was to show that the proposed 3D hybrid beamforming performs pretty well in real environments. To evaluate the system level performance gain, we developed Wireless System Engineering (WiSE). Five small cell BSs were deployed on the second and third floors respectively according to the locations shown in Fig.4(a).

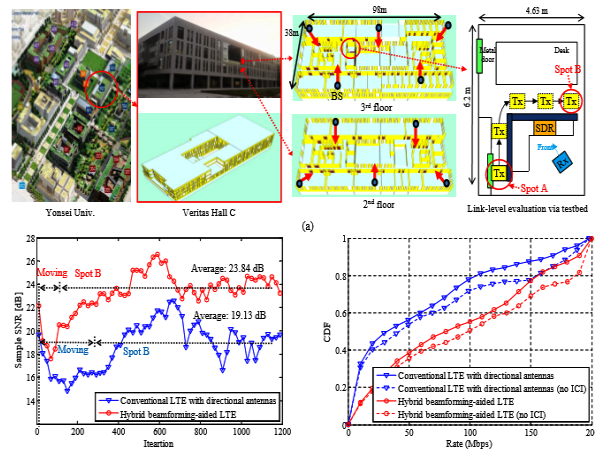


Fig.4.

The downlink rate evaluation per mobile station (MS) was then carried out. The MSs were uniformly distributed on every floor of the buildings and they were associated with the cell that provided the strongest SNR. For the proposed hybrid beamforming-aided LTE system, we assumed that the uplink beam weight is reciprocal to the downlink beam weight, and the BS used the saturated beam weight. For both systems, the small cell BSs had two transmit RF chains and the MSs had two receive RF chains. For the proposed hybrid beamforming-aided LTE, the number of RF chain was two and the size of the subarray was 6×2 as described in Fig. 2(c), i.e., $M = 2$ and $N = 12$. Each cell randomly scheduled one MS in the coverage and



performed single-user MIMO with spatial multiplexing (LTE Transmission Mode 4). Figure 5(c) illustrates the cumulative density function of the ergodic achievable rate of the MSs. When the transmit power of the BSs was 23 dBm. The system parameters follow the LTE specifications where the system bandwidth was 20 MHz; thus the maximum data rate is 200 Mbps [9]. We also depicted the achievable rates of both systems while assuming no ICI. The average rates of the conventional LTE system and the 3D hybrid beamforming-aided LTE system were 56.97 Mbps and 89.04 Mbps respectively. This gave rise to an enhanced rate performance, approximately 56% on average, for the entire service area.

Cho, K. Cheun, and F. Aryanfar, "Millimeter-wave beamforming as an enabling technology for 5G cellular communications

V. CONCLUSION

This article has proposed a smart small cell concept to play a key role in supporting 5G networks, in which a user-specific 3D hybrid beamforming. In this article, we first validated the feasibility of the proposed 3D hybrid beamforming by implementing a real-time SDR testbed. Based on the measured data through the SDR testbed, we also performed 3D ray-tracing-based system-level simulations to investigate the system-level potential gain of the proposed smart small cell system. We expect our prototype design to provide worthwhile insights into developing the most viable solution for future wireless communication systems with an in-depth consideration of practical implementation.

ACKNOWLEDGMENT

I would like to thank the all library media specialists for their participation in the survey who supported my work in this way and helped me get results of better quality. I am also grateful to the members of my group members for their patience and support in overcoming numerous obstacles.

REFERENCES

- [1] Cisco Visual Networking Index, "Cisco Visual Networking Index: Global Mobile Data Traffic Forecast Update, 2014–2019," Feb. 2015.
- [2] ICT-317669 METIS project, "METIS final project report," Del. D8.4, Apr. 2015.
- [3] 5G Forum, "5G Vision, Requirements, and Enabling Technologies," V.1.0, Feb. 2015.
- [4] J. Andrews, F. Baccelli, and R. Ganti, "A tractable approach to coverage and rate in cellular networks," *IEEE Trans. Comm.*, vol. 59, no. 11, pp. 3122–3134, Nov. 2011.
- [5] Y. Kim, H. Ji, J. Lee, Y.-H. Nam, B. L. Ng, I. Tzanidis, Y. Li, and J. Zhang, "Full dimension MIMO (FD-MIMO): The next evolution of MIMO in LTE systems," *IEEE Wireless Comm. Mag.*, vol. 21, no. 3, pp. 92–100, Jun. 2014.
- [6] C.-B. Chae, I. Hwang, R. W. Heath, Jr., and V. Tarokh, "Interference aware-coordinated beamforming in a multi-cell system," *IEEE Trans. Wireless Comm.*, vol. 11, no. 10, pp. 3692–3703, Oct. 2012.
- [7] X. Huang, Y. Guo, and J. Bunton, "A hybrid adaptive antenna array," *IEEE Trans. Wireless Comm.*, vol. 9, no. 5, pp. 1770–1779, May 2010. [8] W. Roh, J.-Y. Seol, J. Park, B. Lee, J. Lee, Y. Kim, J.